ONLINE APPENDIX

1. Detailed Supplemental Text:

Experimental models and experimental designs

All procedures were approved by the Institutional Care and Use Committee of the University of Pennsylvania and Eli Lilly and Company. Adult male C57BL/6 mice (Taconic) weighing ~20g at arrival (n=84) were housed under a 12-hour:12-hour light/dark cycle in a temperature- and humidity- controlled vivarium. Mice were individually housed in standard cages with *ad libitum* access to chow diet (2014, Research Diets) and tap water for all experiments except when noted.

Adult male Sprague-Dawley rats (Charles River) weighing ~250-270 g (n=93) at arrival were housed under a 12-hour:12-hour light/dark cycle in a temperature- and humidity- controlled vivarium. Rats were individually housed in hanging wire-bottomed cage with *ad libitum* access to chow diet (Purina Lab Diet 5001), tap water and also had *ad libitum* access to kaolin pellets (Research Diets, K50001). Rats were exposed to kaolin for at least 5 days prior to measuring kaolin consumption in pica testing.

Adult male shrews (*Suncus murinus*) weighing ~50-80 g (n=118 total), where bred and maintained in the De Jonghe Lab (University of Pennsylvania). These animals were offspring from a colony previously maintained at the University of Pittsburgh Cancer Institute (Dr. Charles Horn); a Taiwanese strain derived from stock originally supplied by the Chinese University of Hong Kong). Shrews were single housed in plastic cages (37.3 x 23.4 x 14 cm, Innovive) under a 12-hour:12-hour light/dark cycle in a temperature- and humidity- controlled environment. Animal were fed *ad libitum* with a mixture of feline (75%, Laboratory Feline Diet 5003, Lab Diet) and mink food (25%, High Density Ferret Diet 5LI4, Lab Diet) and had *ad libitum* access to tap water except where noted.

Animals were habituated to single housing in their home cage and IP injections at least 1 wk prior to experimentation. All animals were naïve to experimental drugs and test prior to the beginning of the experiment. For most *in vivo* experiments, injections were administered using a within-subjects, Latin square design. The exceptions were the conditioned avoidance studies in mice, the glucose tolerance tests in rodents, and the immunohistochemical studies in shrews, which were conducted in a between-subjects design. In all experiments employing a within-subject design, all experimental injections were separated by at least 96 h. Injections were performed shortly before dark-onset, except when noted. Power analyses were performed ahead according to a model of 20% minimum effect size (α=0.05, β=0.10) for kaolin/food intake, with estimated standard deviation based on our published work.

Peptide synthesis and *in vitro* characterization

Long-acting GIPR (GIP-085), the short acting GIPR (GIP-532) and the long-acting GLP-1R agonist GLP-140 were synthesized at Eli Lilly and Company. Cyclic adenosine monophosphate (cAMP) assays were conducted in HEK293 cells expressing the rat GLP-1R, GIPR, or glucagon receptor (GcgR). Using Homogeneous Time Resolved Fluorescence methods to assess cAMP accumulation (CisBio cAMP Dynamic 2 HTRF Assay Kit, 62AM4PEJ), assays were conducted to determine the potency of GIP-085 and GLP-140 performed in the presence of casein (instead of serum albumin) as a nonspecific blocker, which does not interact with the fatty acid moiety of GIP-085 and GLP-140. Intracellular cAMP levels were determined by extrapolation using a standard curve. Dose response curves of compounds were plotted as the percentage of stimulation normalized to minimum (buffer only) and maximum (maximum concentration of each control ligand) values and analyzed using a four-parameter non-linear regression fit with a variable slope (Genedata Screener 13). EC_{50} is the concentration of compound causing half-maximal simulation in a dose response curve.

Drugs and route of administration, and related study design

GIP-085 and GLP-140 were dissolved in 40 mM Tris HCl buffer (pH 8) 0.02% Tween-80. Ex4 and LiCl (0.3M) were dissolved in saline. For the study in mice, all drugs were injected subcutaneously (SC) at a volume of 5 ml/kg of body weight, except LiCl that was injected at 20 ml/kg. In rats, all drugs were injected intraperitoneally (IP), at a volume of 1 ml/kg of body weight, except when noted. In shrews, all drugs were injected IP at a volume of 10 ml/kg of body weight.

Pharmacokinetic analysis

The pharmacokinetics of GIP-085 and GLP-140 was evaluated in rats following a single intravenous (IV) or subcutaneous (SC) dose of 50 nmol/kg. Blood samples were collected over 168-hours. Plasma was harvested from the blood samples by centrifugation and stored frozen until analysis by liquid chromatography with mass spectrometry methods. The resulting individual concentrations from n=2-3 animals were used to calculate the PK parameters. The PK profiles and mean PK parameters are shown in (**Figure 1**).

Effects of GIP-085 systemic delivery on Ex4 conditioned flavor/taste avoidance in mice

The saccharin two bottles test was performed as described elsewhere (*1*). Briefly, C57Bl/6 mice (n=84) were habituated for a week with two H_2O bottles prior to starting the assay. After an overnight H_2O deprivation, animals were given access to a 0.15% saccharin solution in 2 water bottles for approximately 40 minutes. Immediately afterwards, animals were assigned to one of 13 experimental conditions and injected with vehicle or GIP-532 (3 nmol/kg), followed by Ex4 at 0.3, 1, 3, 10, 30 nmol/kg or vehicle. Two days after, animals were water-deprived overnight in preparation for the 2-bottle choice test. The following day animals were tested for expression of conditioned taste avoidance (CTA) by providing them access to 1 bottle of H_2O and 1 bottle of

0.15% saccharin solution and measuring fluid intake during a 24h access period (bottle placement was randomized to prevent place preference) sides switched at 45 min to minimize side preference).

Effects of GIP-085 on glycemic control and insulin levels in rats

The paradigm for the IPGTT in rats was the same as described in mice. Rats (n=6 per group) were injected with GIP-85 (10, 30, 100, 300 nmol/kg) or vehicle. At 0-, 15-, 30- and 60-min extra tail blood was collected for the analysis of circulating insulin levels. Blood was collected in EDTA coated tubes.

Effects of systemic GIP-085, GLP-140 and GIP/GLP-140 dual treatment on food and kaolin consumption, and body weight in rats

Kaolin intake (i.e., pica, a well-established as a model of nausea in rats (*2*)) was measured in addition to food intake. Rats (n = 18, 300-350 g) received an IP administration of GIP-085 (300 nmol/kg), GLP-140 (1000 nmol/kg), GIP-085/GLP-140 combo or vehicle. Food and kaolin intake were measured at 1, 3, 6, 24 h post-injection and body weight was measured at 0 and 24h. A within-subject paradigm was used, with each round of injections separated by 7 days. Rats were stratified into injection treatment groups by body weight.

Effects of brainstem GIPR agonism on GLP-140-induced anorexia, pica and body weight loss in rats

Rats (n=15, 300-350 g) were implanted with an indwelling cannula targeting the 4^{th} ventricle as previously described (*3*). After recovery, the short acting GIP-532 (0.3 nmol in 1µl) or vehicle was infused into the 4^{th} ventricle while GLP-140 (1000 nmol/kg) or vehicle was administered IP. Food and kaolin intake were measured at 3, 6, 24 h post-injection and body weight was measured at 0 and 24h. A within-subject paradigm was used, with each round of injections separated by 7 days.

Dose-response effects of GIP-085 and GLP-140 on glycemic control in shrews

The protocol for performing an intraperitoneal glucose tolerance test (IPGTT) in shrews was previously described (*4, 5*). Briefly, three hours before dark onset, shrews were food- and water-deprived. Two hours later, baseline blood glucose levels were determined from a small drop of tail blood and measured using a standard glucometer (AccuCheck). Immediately following, each shrew (n=10) received IP injection of GIP-085 (3, 30, 300, 3000 nmol/kg) or vehicle (1 mL/100g BW). BG was measured 30 minutes later (t = 0 min), then each shrew received an IP bolus of glucose (2 g/kg). Subsequent BG readings were taken at 20, 40, 60 and 120 min after glucose injection. After the final BG reading, food and water were returned. IPGTT was carried out in a between-subject design. In another cohort of animals (n=9) the same paradigm was applied in which each shrew received IP injection of GLP-140 (30, 300, 1000, 3000 nmol/kg) or vehicle. This study was conducted in a within-subject, counter-balanced design, with each round of injections separated by 7 days.

Direct comparison of GLP-140, GIP-085 and GIP-085/GLP-140 treatment on glycemic control in shrews

IPGTT in shrews (n=15) was performed as described above for rats, with GLP-140 (1000 nmol/kg), GIP-085 (300 nmol/kg) GIP-085/GLP-140, or vehicle being injected. This experiment was conducted in a within-subject, counter-balanced design with each round separated by 5 days.

Dose-response effects of GIP-085 on energy balance in shrews

We evaluated the effects on food intake and body weight of different doses of GIP-085. Food was removed 2h prior to dark onset. Shortly before dark onset shrews (n=10) received IP injection of GIP-085 (300, 3000 nmol/kg), or vehicle. Shrews had *ad libitum* access to powdered food through a circular (3 cm diameter) hole in the cage. Food intake was evaluated using our custom-made

feedometers, consisting of a standard plexiglass rodent housing cage (29 x 19 x 12.7 cm) with mounted food hoppers resting on a plexiglass cup (to account for spillage). Food intake was manually measured at 6, 24, 48 and 72h post injection. Body weight was taken at 0, 24, 48 and 72h. Treatments occurred in a within-subject, counter-balanced design and were 4 days apart.

Effects of GLP-140 on energy balance in shrews

In shrews (n=8) the effects of GLP-140 (1000 nmol/kg) or vehicle on food intake and body weight were evaluated as described above. Treatments occurred in a within-subject, counter-balanced fashion and were 7 days apart.

Direct comparison of GLP-140, GIP-085 and GIP-085/GLP-140 treatments on energy balance in shrews

We then compare the effects of GLP-140 (1000 nmol/kg), GIP-085 (300 nmol/kg) GIP-085/GLP-140, or vehicle in the same animals (n=10) using in a within-subject, counter-balanced design. This experiment was conducted as described above. Each treatment was 7 days apart.

Emetogenic properties of different dose of GIP-085 and GLP-140 in shrews

First, shrews (n=10) were habituated to IP injections and to clear plastic observation chambers (23.5 x 15.25 x 17.8 cm) for two consecutive days prior to experimentation. The animals were injected IP with GIP (300, 3000 nmol/kg), or vehicle, then video-recorded (Vixia HF-R62, Canon) for 120 minutes. After 120 min, the animals were returned to their cages. Treatment rounds were conducted within-subject and separated by 3 days. In a second group of shrews (n=10), IP injections of GLP-140 (30, 300, 1000, 3000 nmol/kg) or vehicle were performed. Treatments were separated by 7 days and administered in a within-subject manner. Analysis of emetic episodes were measured by an observer blinded to treatment groups. Emetic episodes were characterized by strong rhythmic abdominal contractions associated with either oral expulsion from the

gastrointestinal tract (i.e. vomiting) or without the passage of materials (i.e. retching). Latency to the first emetic episode, total number of emetic episodes and number of emetic episodes per minute were quantified.

Direct comparison of GLP-140, GIP-085 and GIP-085/GLP-140 treatments on emesis in shrews

Shrews (n=10) were habituated to the experimental conditions as described above. The animals were injected IP with GLP-140 (1000 nmol/kg), GIP-085 (300 nmol/kg) GIP-085/GLP-140, or vehicle, then video-recorded (Vixia HF-R62, Canon) for 120 minutes. After 120 min, the animals were returned to their cages. Treatments were separated by 5 days. Analysis of emetic episodes were measured by an observer blinded to treatment groups. Emesis parameters were quantified as described above. The same experimental paradigm was also repeated in a separate group of animals (n=9).

Assessment of neuronal activation in the DVC following GLP-140, GIP-085 and GIP-085/GLP-140 treatments in shrews

Body weight-matched shrews (n=19) received IP injection of GIP-085 (300 nmol/kg, n=4), GLP-140 (1000 nmol/kg, n=5), GIP-085/GLP-140 combo (n=7) or vehicle (n=3) just prior to dark onset. Food was removed to avoid feeding-related changes in c-Fos expression between groups. 90 min later, shrews were deeply anesthetized with IP triple cocktail of ketamine, xylazine and acepromazine (180 mg/kg, 5.4 mg/kg and 1.28 mg/kg; respectively) and transcardially perfused with 0.1M PBS (Boston Bioproducts), followed by 4% PFA (in 0.1M PBS, pH 7.4, Boston Bioproducts). Brains were removed and post fixed in 4% PFA for 48h and then stored in 25% sucrose for two days. Brains were subsequently frozen in cold hexane and stored at -20°C until further processing. Thirty micrometer-thick frozen coronal sections containing the DVC were cut in a cryomicrotome (CM3050S, Leica Microsystem), collected and stored in cryoprotectant (30%

sucrose, 30% ethylene glycol, 1% polyvinyl-pyrrolidone-40, in 0.1M PBS) at -20°C until further processing. IHC was conducted according to previously described procedure (*4, 5*). Briefly, free-floating sections were washed with 0.1M PBS (3x8min), incubated in 0.1M PBS containing 0.3% Triton X-100 (PBST) and 5% normal donkey serum (NDS) for 1h, followed by an overnight incubation with rabbit anti-Fos antibody (1:1000 in PBST; s2250; Cell Signaling,). After washing (3x8min) with 0.1M PBS sections were incubated with the secondary antibody donkey anti-rabbit Alexa Fluor 488 (1:500 in 5% NDS PBST; Jackson Immuno Research Laboratories,) for 2h at room temperature. After final washing (3x8min in 0.1M PBS) the sections were mounted onto glass slides (Superfrost Plus, VWR) and coverslipped with Fluorogel (Electron Microscopy Sciences). c-Fos positive neurons spanning the DVC were visualized (20x; Nikon 80i, NIS Elements AR 3.0) and quantified (FIJI software) using fluorescence microscopy. A total of 3 DVC sections per animal were used to quantify the number of c-Fos labeled cells in the AP and NTS (~200-250 µm rostral to the obex), similarly as previously described (*4, 5*) by an experimenter blinded to the treatment.

Identification and characterization of GIPR neurons in the AP/NTS via Fluorescent In-Situ Hybridization (FISH) in rats

Rats (n=4, ~400 g) were deeply anesthetized with IP triple cocktail of ketamine, xylazine and acepromazine (180 mg/kg, 5.4 mg/kg and 1.28 mg/kg; respectively) in the middle of the dark-phase. Brains were removed and snap-frozen in dry ice-cold hexane. Twenty µm-thick hindbrain coronal sections containing the AP/NTS were obtained using a cryostat (Leica, CM3050S), slide-mounted and stored at -80°C until further processing. AP/NTS sections were used to perform FISH using a commercially available kit (Cat. No. 320851 RNAscope Fluorescent Multiplex Detection Reagent Kit, Advanced Cell Diagnostics) according to the manufacturer's instructions. Briefly, sections were fixed in 4ºC 10% NBF for 15 min. Slides were washed 2x with 1x PBS and dehydrated in ascending ethanol solutions (5 min washes in 50, 70, 100, 100% ethanol). After the

second 100% ethanol wash, slides were air-dried, and a hydrophobic barrier was created on the slide surrounding the sections. The sections were treated with Protease IV and incubated for 30 min at room temperature. Next, slides were rinsed with 1x PBS twice and then incubated for 2h at 40^{o}C using ACD probes for GLP-1R, GIPR and GFRAL mRNA. Following incubation, slides were rinsed twice with 1X wash buffer before being treated with a series of amplification steps at 40^{o}C: 30 min incubation in AMP1-FL, 15 min incubation in AMP2-FL, 30 min incubation in AMP3-FL, 15 min incubation in AMP4-FL (with two rinses in wash buffer between each step). Following the amplification steps the sections were counterstained with DAPI and coverslipped with ProLong Gold Antifade Mountant. Slides were stored at 4 ^{o}C and imaged 24 h later.

AP/NTS transcriptome profile of single nuclei in rats

Tissue collection: Rats (n=4, ~400 g) were deeply anesthetized with IP triple cocktail of ketamine, xylazine and acepromazine (180 mg/kg, 5.4 mg/kg and 1.28 mg/kg; respectively) in the middle of the dark-phase. Brains were removed and snap-frozen in dry ice-cold hexane. Three adjacent micro-punch samples (each 1 cubic mm) containing the AP and left and right NTS were collected from coronally-prepared brains on a cryostat, pooled together and stored at -80°C until further processing.

Isolation of Nuclei: Nuclei were isolated from frozen AP and NTS punches, similar to a previous description (*6, 7*). AP and NTS tissue punches from a single animal were dounce homogenized together in 0.5 mL lysis buffer (nuclease-free water with 10 mM Tris-HCL, 10 mM NaCl, 3 mM $MgCl_2$, 0.5% NP-40) using 20 strokes of the loose pestle and 10 strokes of the tight pestle. The homogenate was diluted to 2.5 mL with lysis buffer and left to lyse on ice for an additional 5 minutes, followed by addition of an equal volume of wash buffer (1X PBS with 2% BSA, 1:1000 RNase inhibitor, 0.25% Glycerol). Samples were then passed through a 30 µm cell strainer and centrifuged at 500 x g for 7 minutes at 4°C. Supernatants were decanted and pellets were

resuspended in 3 mL wash buffer. Samples were passed through a 30 µm cell strainer for a second time and centrifuged at 500 x g for 10 minutes at 4°C. Supernatants were decanted and pellets were resuspended in 1.5 mL wash buffer and centrifuged at 500 x g for 10 minutes at 4°C. Supernatants were decanted and pellets were resuspended in 50 µL wash buffer. Nuclei were counted by the Trypan Blue method using a hemocytometer and resuspended in wash buffer at a concentration of 1,000 nuclei/µL.

10x Library Preparation and Sequencing: Microfluidics capture and sequencing library preparation was performed with the 10x Genomics Chromium Single Cell 3' GEM, Library and Gel Bead Kit v3.1 at the Children's Hospital of Philadelphia Center for Applied Genomics per manufacturer's instructions. Target capture was ~10,000 nuclei per sample. Unique dual indexed sequencing libraries were prepared per manufacturer protocols, and the libraries were sequenced on an Illumina NovaSeq 6000.

QC and Clustering: 10x Genomics Cell Ranger v3.1 was used to align reads to the rat pre-mRNA transcriptome (Rattus_norvegicus.Rnor_6.0.101). Filtered read count matrices for all animals were merged using Seurat version 3.1. The distributions of the numbers of genes and unique molecular identifiers (UMIs) were assessed to identify potential outliers. Nuclei in the bottom 0.5% for number of genes (< 532) were removed due to likely being uninformative, similar to prior reports (*6, 8-10*). Nuclei in the top 0.5% of gene count (> 4,535) and/or top 1% of UMI count (> 9,794) were removed as putative multiplets, also similar to previous reports (*6, 8-10*). Finally, as previously described, nuclei in which >5% of transcripts were of mitochondrial origin were removed and all mitochondrial transcripts were removed from the data set (*11*).

Counts were normalized to 10,000 counts per subject and scaled in Seurat. Variably expressed genes were identified with the FindVariableFeatures function in Seurat using the mean.var.plot selection method and analyzing only genes with mean scaled expression between 0.003 and 2.

These parameters identified 1,133 highly variable genes, which were used to generate principal components (PCs). Clustering was performed in Seurat using the first 50 PCs, generating 27 clusters at a resolution of 0.25. Six clusters were represented in only 2 of the 4 samples, with three of these clusters expressing *Slc17a7* (VGLUT1), a gene that is not present in the AP or NTS. These six clusters likely represent capture of adjacent brain stem regions and were removed.

Annotation of Cell Clusters: Major cell types were identified using known markers of major cell types (*6*): Microglia: - *Cx3cr1*, *Mrc1*; Endothelial – *Cldn5*; Astrocytes – *Cldn10*, *Glul*, *Aqp4*; Oligodendrocyte Precursor Cells – *Pcdh15*, *Pdgfra*, *Olig1*, *Olig2*; Oligodendrocytes – *Mag*, *Mog*, *Plp1*, *Mobp*, *Mbp*; Excitatory Neurons – *Slc17a6*; Inhibitory Neurons – *Gad1*, *Gad2*, *Slc32a1*; Neurons – *Snap25*, *Stmn2*; Tanycytes – *Vim* (*12*); Ependymocytes – *Cfap52*, *Vim* (*12*); Radial Glia – *Notch2* (*13*), *Slc1a3* (*14*). Two clusters with mixed major cell type markers were removed for a final total of 19 clusters.

Statistical analysis

Body weight changes were calculated by subtracting body weight on any given post-treatment day from the rat's weight on the day of injection. In all behavioral studies, food intake, kaolin intake and body weight changes data were analyzed using ordinary or repeated measures one-way or two-way ANOVAs followed by Tukey's post hoc tests. For the analysis of c-Fos expression an ordinary one-way ANOVA was used, followed by Tukey's post hoc tests. BG levels were analyzed using ordinary or repeated measures Two-Way ANOVA followed by Tukey's post-hoc test. AUCs were calculated from 0 to 120 min using the trapezoidal method. Resulting AUCs were analyzed using ordinary or repeated measures One-Way ANOVA followed by Tukey's post-hoc test. All data were expressed as mean ± SEM. For all statistical tests, a *p*-value less than 0.05 was

considered significant. Information on replicates and significance is reported in the figure legends. All data were analyzed using Prism 9 GraphPad Software (San Diego, California).

Data Availability

Single nuclei RNA sequencing data are available at the NCBI Gene Expression Omnibus (GEO) under accession number GSE167981. Except for the raw RNA sequencing dataset, the published article includes all data generated or analyzed during this study.

2. Supplementary Figures and tables

Supplementary Figure 1

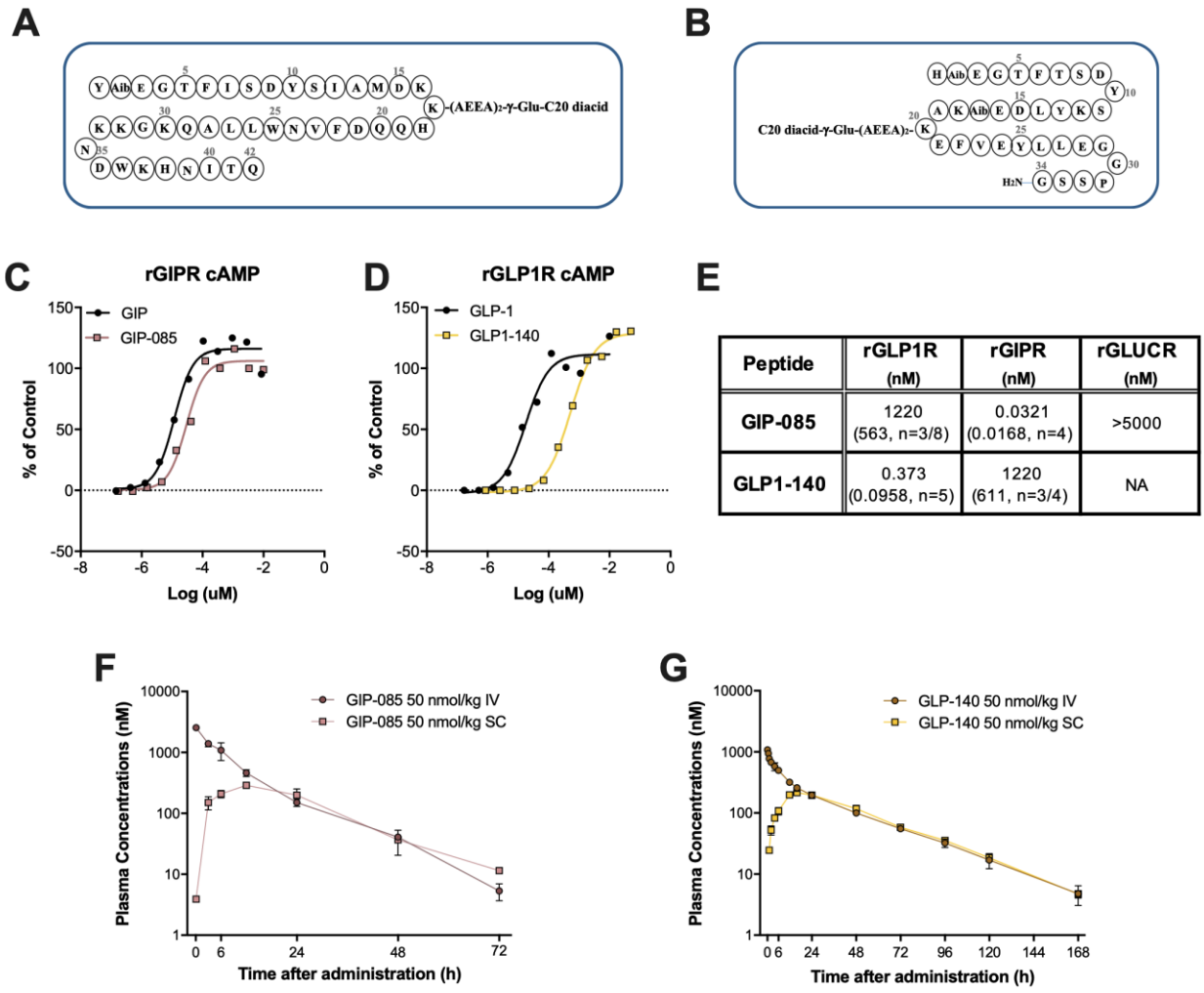

Peptide	rGLP1R (nM)	rGIPR (nM)	rGLUCR (nM)
GIP-085	1220 (563, n=3/8)	0.0321 (0.0168, n=4)	>5000
GLP1-140	0.373 (0.0958, n=5)	1220 (611, n=3/4)	NA

Supplementary Figure 1: Generation and *in vitro* characterization of the long acting GLP-1R and GIPR agonists GLP-140 and GIP-085

A) Structure schematic of a long-acting glucose-dependent insulinotropic polypeptide receptor agonist (GIP-085).

B) Structure schematic of a long-acting glucagon-like peptide 1 receptor agonist (GLP-140).

C) Representative concentration response curves (cAMP accumulation) of GIP-085.

D) Representative concentration response curves (cAMP accumulation) of GLP-140.

E) in vitro potency (EC50) by GIP-085 and GLP-140 in HEK293 cells expressing the rat GIPR, GLP-1R and GcGR.

F) Plasma profile after administration of GIP-085 follow a single IV or SC dose (50 nmol/kg) in male Sprague Dawley rats.

G) Plasma profile after administration of GLP-140 follow a single IV or SC dose (50 nmol/kg) in male Sprague Dawley rats.

All data are presented as mean ± SEM.

Supplemetary Figure 2

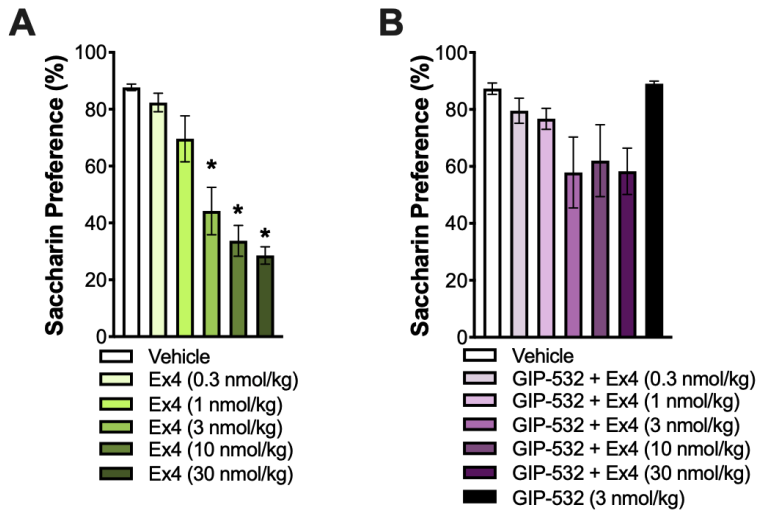

Supplementary Figure 2. GIPR agonism attenuates conditioned taste avoidance (CTA) in mice to saccharin induced the GLP-1 analog Exendin-4 (Ex4) (related to Fig. 1)

A) The GLP-1 analog Exendin 4 (Ex4) induces conditioned taste avoidance (CTA) in a dose-dependent fashion (n=6 per group).

B) GLP-1R agonist-induced CTA was prevented following non-lipidated GIPR agonist GIP-532 co-treatment (3 nmol/kg) in all doses tested.

All data expressed as mean ± SEM. Data were analyzed with one-way ANOVA followed by Tukey's post hoc test. Means with different letters are significantly different from each other ($P < 0.05$).

Supplementary Figure 3

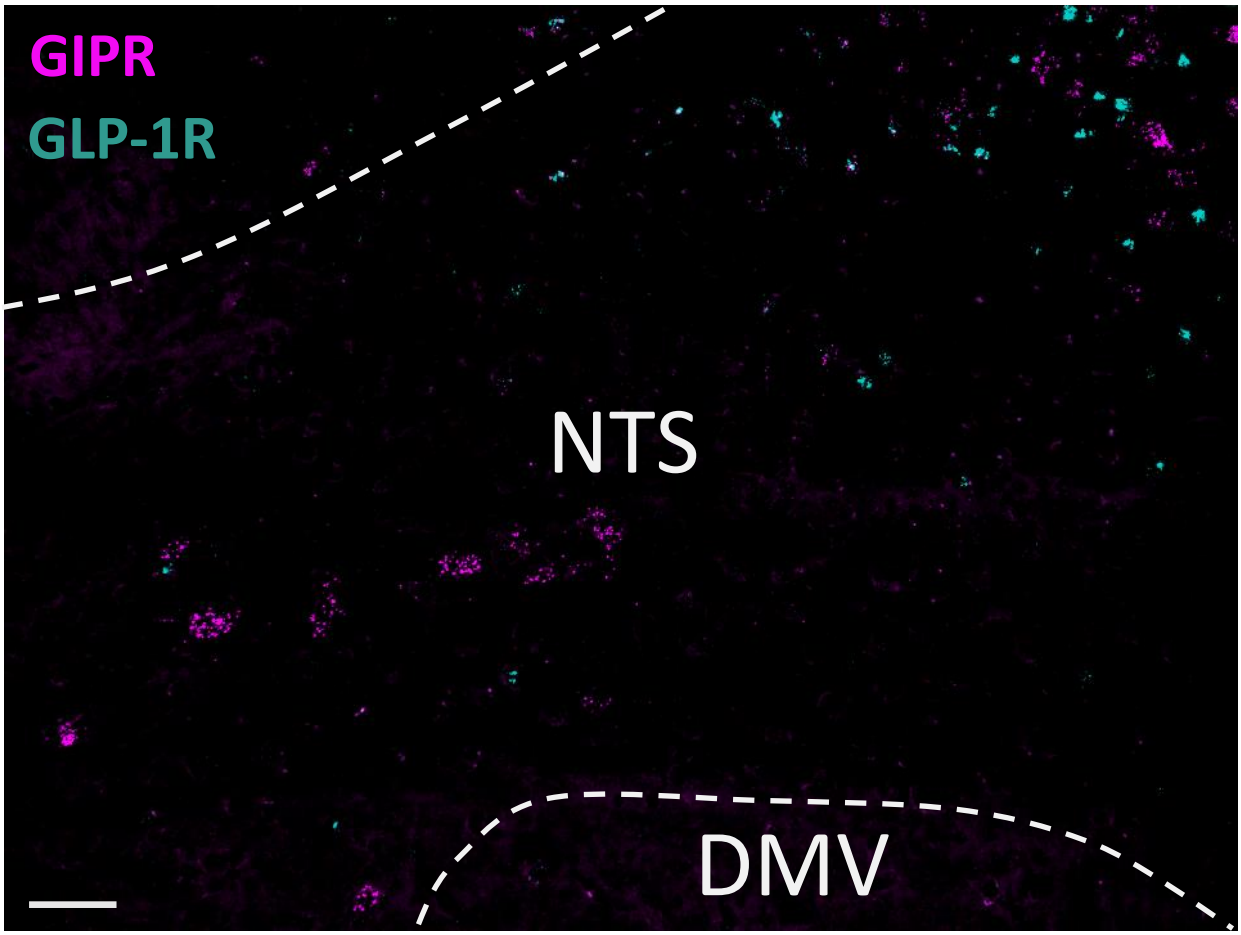

Supplementary Figure 3: FISH NTS (related to Fig. 2)

Representative Fluorescent In-Situ Hybridization (FISH) images showing $Gipr^{+}$and $Glp1r^{+}$ cells in the left NTS of the rat (~250 µm rostral to the obex). Scale bar 50µm.

Supplemetary Figure 4

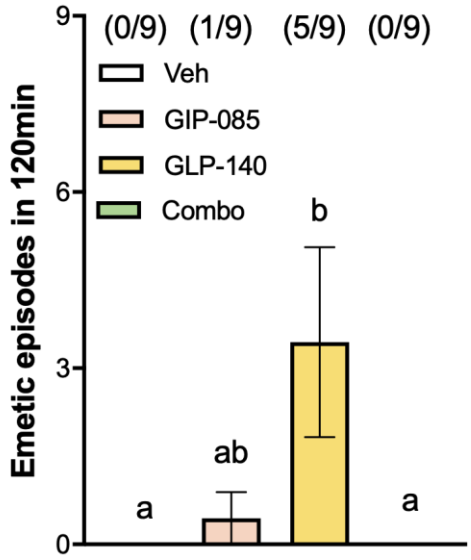

Supplementary Figure 4. GIP-085 completely prevents GLP-140-induced emesis in shrews (related to Fig. 4)

The anti-emetic effects of GIP-085 treatment were tested again in a separate cohort of shrews (n=9). Similar to **Fig. 4E**, GLP-140 (1000 nmol/kg) induced severe emesis that was completely prevented by GIP-085 (300 nmol/kg) co-treatment. Data expressed as mean ± SEM and analyzed with repeated measures one-way ANOVA followed by Tukey's post hoc test. Means with different letters are significantly different from each other ($P < 0.05$).

S. Table 1:

Summary of the mean pharmacokinetic parameters following administration of a single intravenous (IV) or subcutaneous (SC) dose of GIP-085 (50 nmol/kg, n=2/route) or GLP-140 (50 nmol/kg, n=3/route) in rats.

	GIP-085		GLP-140	
	IV	**SC**	**IV**	**SC**
Dose (nmol/kg)	50	50	50	50
C_{max} (nmol/L)	-	288	-	217
T_{max} (h)	-	12.0	-	17.3
AUC_{INF} (h*nmol/L)	19628	8036	16810	11868
Vd (IV) or **Vd/F (SC)** (mL/kg)	34.8	96.8	113	150
CL (IV) or **CL/F (SC)** (mL/h/kg)	2.56	6.32	3.00	4.22
$T_{1/2}$ (h)	9.47	10.7	26.4	24.6
%F	-	40.9	-	70.6

AUC_{INF}: Area under the curve from 0 to infinity; CL: clearance; CL/F: apparent clearance; C_{max} = maximal concentration; T_{max} = time at maximal concentration; $T_{1/2}$ = elimination half-life; %F = bioavailability; Vd: volume of distribution; Vd/F: apparent volume of distribution.

Summary of the mean pharmacokinetic parameters following administration of a single intravenous (IV) or subcutaneous (SC) dose of GIP-085 (50 nmol/kg, n=2/route) or GLP-140 (50 nmol/kg, n=3/route) in rats.

3. References related to the Supplemental Text:

1. A. Mansouri *et al.*, Intraperitoneal injections of low doses of C75 elicit a behaviorally specific and vagal afferent-independent inhibition of eating in rats. *Am J Physiol Regul Integr Comp Physiol* **295**, R799-805 (2008).
2. P. L. Andrews, C. C. Horn, Signals for nausea and emesis: Implications for models of upper gastrointestinal diseases. *Auton Neurosci* **125**, 100-115 (2006).
3. T. Borner *et al.*, GDF15 Induces Anorexia through Nausea and Emesis. *Cell Metab* **31**, 351-362 e355 (2020).
4. T. Borner *et al.*, A second-generation glucagon-like peptide-1 receptor agonist mitigates vomiting and anorexia while retaining glucoregulatory potency in lean diabetic and emetic mammalian models. *Diabetes Obes Metab* **22**, 1729-1741 (2020).
5. T. Borner *et al.*, Corrination of a GLP-1 Receptor Agonist for Glycemic Control without Emesis. *Cell Rep* **31**, 107768 (2020).
6. C. Nagy *et al.*, Single-nucleus transcriptomics of the prefrontal cortex in major depressive disorder implicates oligodendrocyte precursor cells and excitatory neurons. *Nat Neurosci*, (2020).
7. B. C. Reiner *et al.* (doi.org/10.1101/2020.07.29.227355, bioRxiv, 2020), vol. doi.org/10.1101/2020.07.29.227355.
8. H. Mathys *et al.*, Single-cell transcriptomic analysis of Alzheimer's disease. *Nature* **570**, 332-337 (2019).
9. L. Schirmer *et al.*, Neuronal vulnerability and multilineage diversity in multiple sclerosis. *Nature* **573**, 75-82 (2019).
10. D. Velmeshev *et al.*, Single-cell genomics identifies cell type-specific molecular changes in autism. *Science* **364**, 685-689 (2019).
11. D. Osorio, J. J. Cai, Systematic determination of the mitochondrial proportion in human and mice tissues for single-cell RNA sequencing data quality control. *Bioinformatics*, (2020).
12. C. Zhang *et al.*, Area Postrema Cell Types that Mediate Nausea-Associated Behaviors. *Neuron* **109**, 461-472 e465 (2021).
13. S. Mase *et al.*, Notch1 and Notch2 collaboratively maintain radial glial cells in mouse neurogenesis. *Neurosci Res*, (2020).
14. A. A. Pollen *et al.*, Molecular identity of human outer radial glia during cortical development. *Cell* **163**, 55-67 (2015).